

SMALL PARTICLE RESPONSE TO FLUID MOTION USING TETHERED PARTICLES TO SIMULATE MICROGRAVITY

James Trolinger^{1*}, Drew L'Esperance¹, Roger Rangel², Carlos Coimbra³,
William Witherow⁴, Jan Rogers⁴, and Ravindra Lal⁵

MetroLaser, Irvine, CA¹, University of California at Irvine², University of Hawaii³,
NASA Marshall Space Flight Center⁴, Alabama A&M University⁵

Abstract

This paper reports on ground based work conducted to support the Spaceflight Definition project SHIVA (Spaceflight Holography Investigation in a Virtual Apparatus). SHIVA will advance our understanding of the movement of a particle in a fluid. Gravity usually dominates the equations of motion, but in microgravity as well as on earth other terms can become important. Through an innovative application of fractional differential equations, two members of our team produced the first analytical solution of a fundamental equation of motion, which had only been solved numerically or by approximation before. The general solution predicts that the usually neglected history term becomes important in particle response to a sinusoidal fluid movement when the characteristic viscous time is in the same order as the fluid oscillation period and peaks when the two times are equal. In this case three force terms, the Stokes drag, the added mass, and the history drag must all be included in predicting particle movement. We have developed diagnostic recording methods using holography to save all of the particle field data, allowing the experiment to essentially be transferred from space back to earth in what we call the “virtual apparatus” for on-earth microgravity experimentation. We can quantify precisely the three-dimensional motion of sets of particles, allowing us to test and apply the new analytical solutions.

We are examining the response of particles up to 2 mm radius to fluid oscillation at frequencies up to 80 Hz with amplitudes up to 200 microns. Ground studies to support the flight development program have employed various schemes to simulate microgravity. One of the most reliable and meaningful methods uses spheres tethered to a fine hair suspended in the fluid. We have also investigated particles with nearly neutral buoyancy. Recordings are made at the peak amplitudes of vibration of the cell providing a measure of the ratio of fluid to particle amplitude. The experiment requires precise location of the particle to within microns during recording, and techniques for achieving this are one of the project challenges. Focused microscopic images and diffraction patterns are used. To make the experiment more versatile, the spaceflight system will record holograms both on film and electronically. A cross correlation procedure enables sub pixel accuracies for electronic recordings, partially accommodating the lower spatial resolution of CCDs. The electronic holograms can be down linked providing real time data. Results of the ground experiments, the flight experiment design, and data analysis procedures are reported.

Keywords: particle dynamics, Stokes flow, microgravity, holography

* Corresponding author e-mail: jtrolinger@metrolaserinc.com

Ground Experiment Objectives and Strategy

Our analytical solution to the particle/fluid equation of motion¹ was used to design both ground and flight experiments that will experimentally test cases that are significantly different from previously approximations and numerical solutions. Our solution shows that the history term cannot be neglected for many interesting cases (especially low Reynolds number cases). A fundamental case that has been selected for study is that of a particle suspended in a fluid that is oscillating sinusoidally. Since the movement of a particle in response to the surrounding fluid is predicted by our solutions, we can test the theory by measuring that response, specifically, the ratio of the particle to fluid amplitude, η and their phase relationship.

The problems of conducting the experiments on earth include particles rising or falling too fast violating the low Reynolds number assumption and the difficulty in locating the particle position with great accuracy when the particle is rising or falling. In a gravitational field as the fluid to particle density ratio, α , approaches unity, the rate of rising or sinking of the particle is small, a precise measurement of particle position is easy to make, and the Reynolds number is small. However, to study the history drag as α approaches unity requires better measurement accuracy because η also approaches unity. Our ground investigation has addressed this in various ways, but the most versatile so far has been a tethered particle method. Particles are tethered on a fiber that holds them in the proper position for recording. This simulates microgravity better, gives much more time, and simplifies recording at the expense of the interference of the tethering fiber. We found this method very effective, although effects from the tethering fiber are observed. The tethering method was used for much of the ground science work.

We have proven in ground experiments that we can locate a particle in a vibrating test cell with a precision sufficient to measure the effect of the history term on the particle amplitude. A specific case that has been tested extensively at MetroLaser is a 1mm-radius polypropylene particle in a Krytox liquid filled cell that is shaken at frequencies up to 100 Hz with amplitude of up to 0.2 mm. The required precision ranges from about 5 microns or better depending on the amplitude of vibration and the value of α . We have run many experiments around the region where the scaling function $S = 1$ (S is the ratio of viscous time to vibration period, and at S equals unity the motion information transfers about one particle diameter during one cycle of oscillation) and with $\alpha = 2.1$. The effect of the history term peaks at about 60 Hz for this case making this an optimum frequency for observing the history term effects. A vibrational amplitude of 100 microns should result in a 15-micron difference with and without the history term. We have shown in our ground experiments that we are at least a factor of two better than the resolution required to quantify the effect.

The objectives of the ground experiments are:

- Establish that the measurement accuracy and resolution required to achieve our project goals are achievable.
- Prove that the flight experiment is feasible with attainable hardware.
- Evaluate the capability of critical hardware components to meet experiment requirements (e.g. laser power and coherence, photographic film properties)
- Support the project science with limited testing of the new solutions to the equations of motion. Test the theory in as wide a range and with as many parameters possible on earth.
- Gain experience and test concepts that will be necessary for conducting a spaceflight experiment.
- Develop data reduction and interpretation methods.
- Identify and resolve critical issues.

Experimental Apparatus Development and Testing^{2,3}

Although the ground experiment is much like the anticipated flight experiment, it has a number of complications that are not expected in microgravity. Figure 1 illustrates the experiment with a free particle rising to the surface.

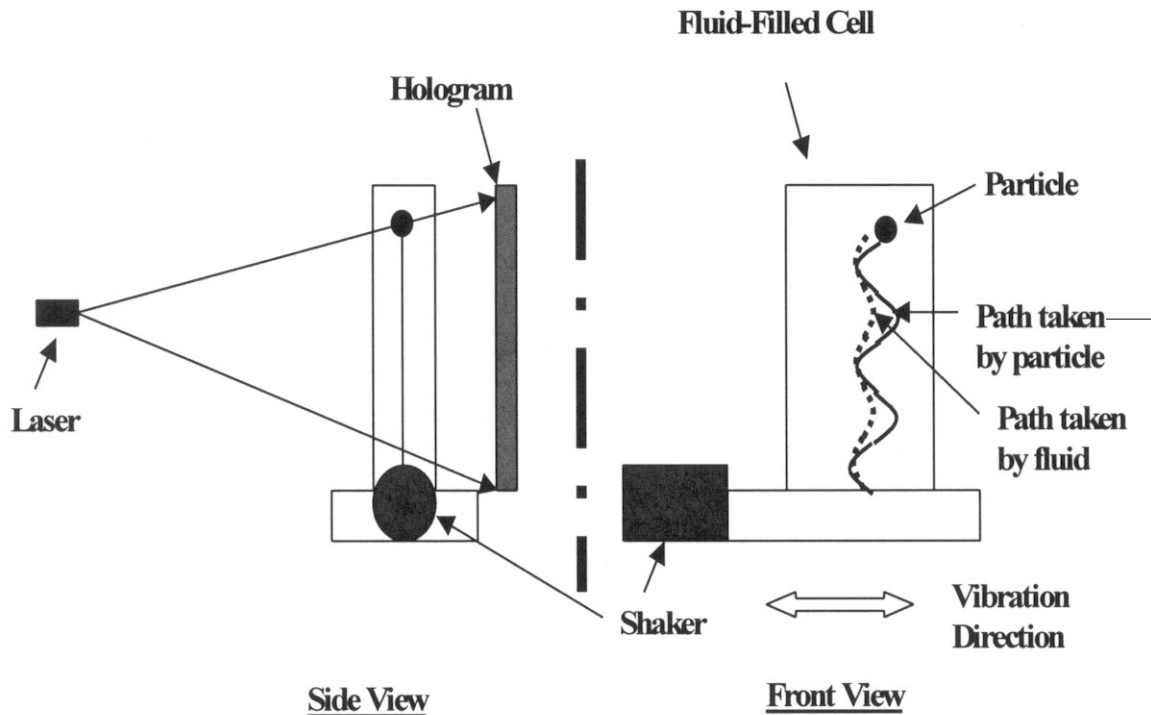


Figure 1. Ground experiment concept.

The problem is to suspend or launch a particle in a fluid filled cell, vibrate the cell along a single axis in a range up to 100 Hz with amplitudes up to ± 200 microns and locate the positions of both the cell and the particle at two different times with micron precision. The cell must be completely filled with fluid at all times during the measurement phase. Particles rise and fall in the fluid under buoyant forces, so there is not much time for observing a free-floating particle. In Figure 1 the particle is released at the bottom of a fluid filled cell, and the fluid is constrained to move with the cell. Therefore, we can measure precisely where the fluid is at all times. As the particle rises, it attempts to follow the sinusoidal movement of the fluid; however, it follows a quasi-sinusoidal path with some phase difference and larger amplitude (see particle and fluid motion in the figure). Our early experiments were done with particles as shown in the figure. The cell design and the particle suspending procedure passed through many evolutions before we arrived at a reliable repeatable experimental apparatus that employed the tethered particle.

Figure 2 shows the ground experimental apparatus. To achieve the required precision and to maintain a single vibration axis it was necessary to mount the cell on a single axis traverse. Tuning and stiffening the apparatus resolved vibrational noise and resonance issues. Removing errors caused by optical system vibration presented a major challenge at the required accuracy. The most reliable choice for a vibrational source was a commercially available electromagnetic shaker (voice coil) that had been selected by the NASA engineering team as a strong candidate for the flight system. It was shown to be entirely effective for the experiment and was eventually adopted as the preferred method for the ground science as well. The

cell holds an approximately four-centimeter cube of fluid between two windows. It provides the ability to test the interaction of particles with the walls and with each other. The cell was designed so that a wall could be moved closer and closer to the particle to evaluate wall effects. In addition, the design allows multiple particles to be tethered and observed.

The system reliably produces vibrational conditions from 30 to 80 Hertz with amplitudes up to 150 microns. So far we have used tethered polypropylene, steel and magnesium, 1 mm radius spheres. We ran a number of tests to determine phase difference in the particle and cell both to measure the effect on our accuracy and also to test the predictions of the theory. We were able to measure the particle phase lead and compared this with theory. The results are within reasonable agreement with the theory.

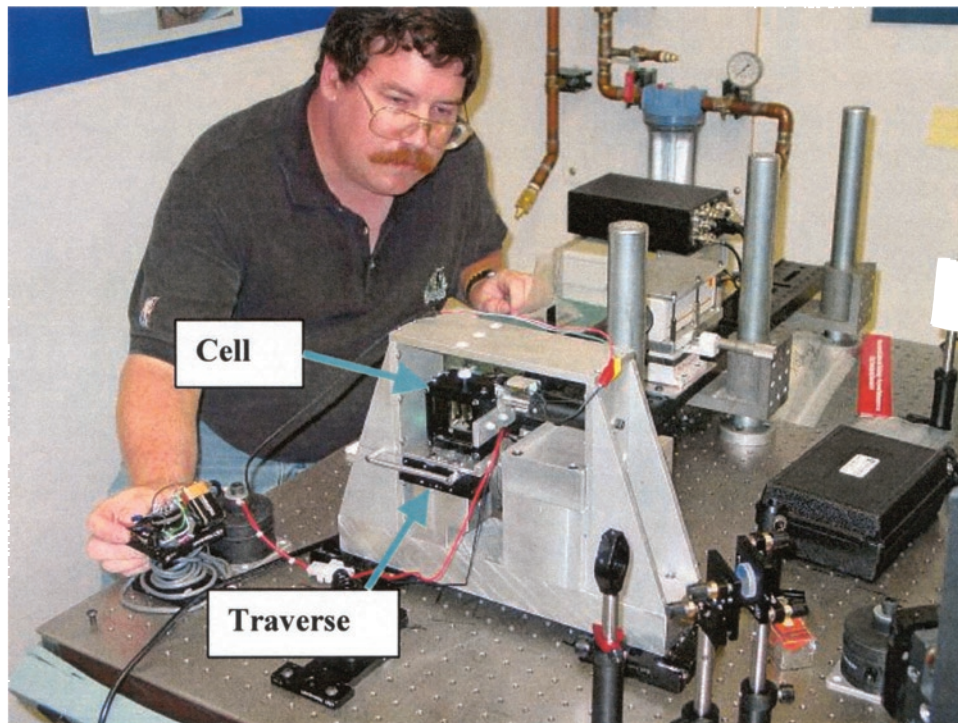


Figure 2 a). Overall view of the ground experiment.

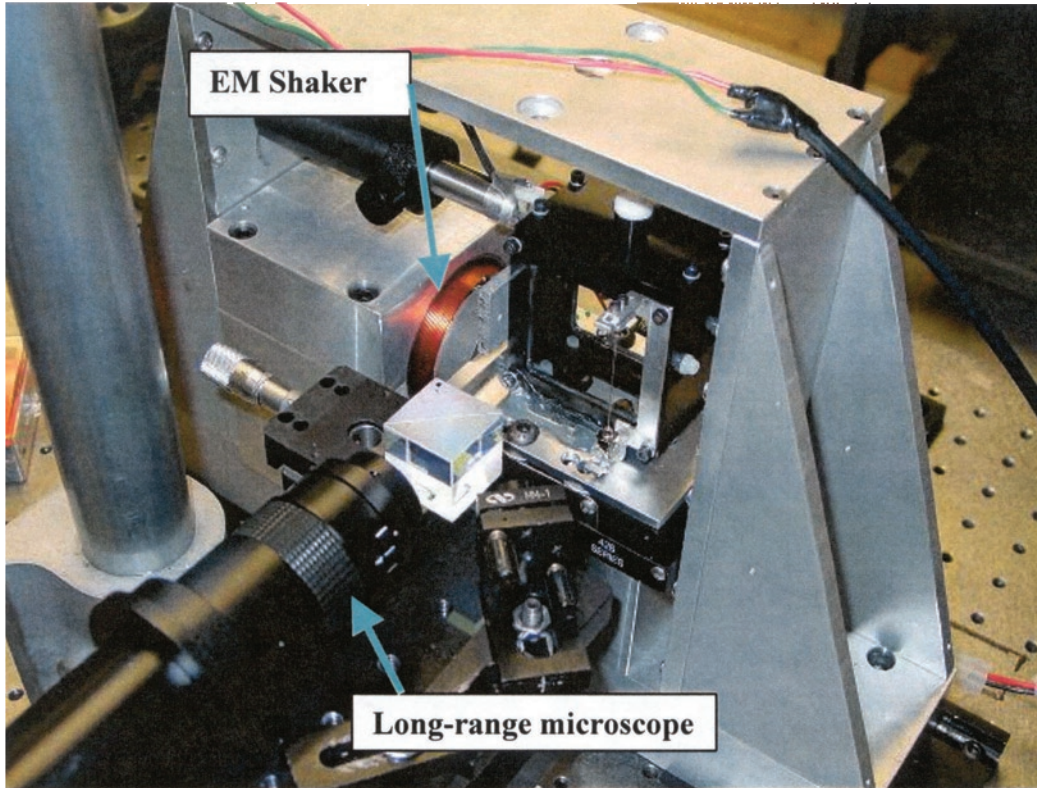


Figure 2 b). Ground cell from long range microscope side.

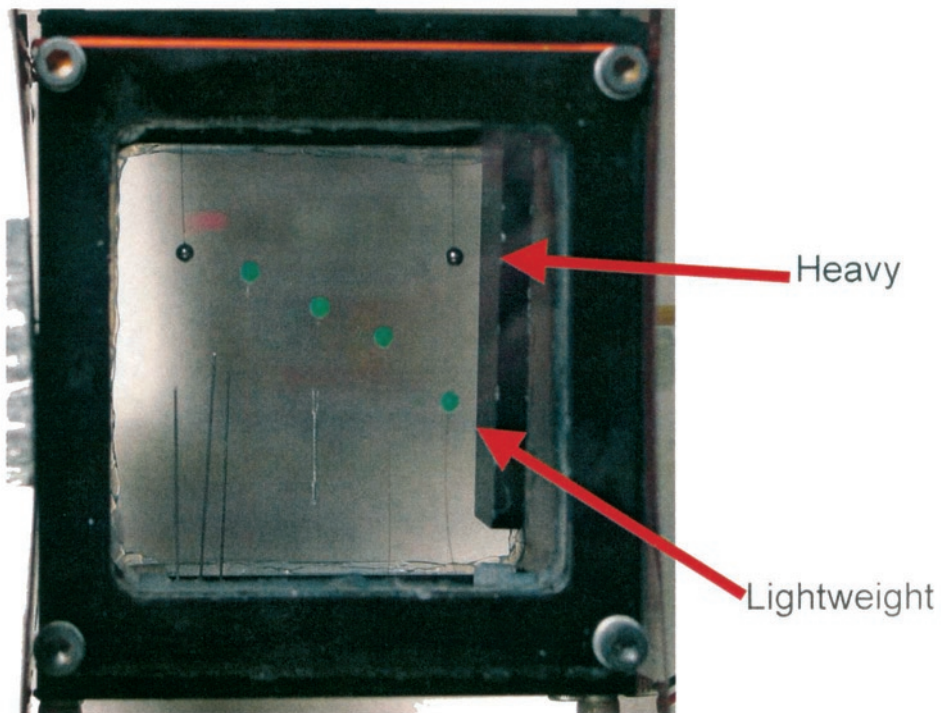


Figure 2 c). Cell showing tethered polypropylene and steel particles (note particles near the wall).

Figure 2. Ground experiment apparatus.

Determining the Ratio of Particle to Fluid Amplitude

To determine the ratio of the particle to fluid amplitude requires that the fluid and particle positions be determined at least at two times in the cycle of vibration. Two measurement methods have been adopted:

1. In the same recording, record two positions of the particle and a reference point on the cell, preferably when the cell positions are at its extremes. This will allow us to make an accurate measurement of the fluid to particle amplitude. The fluid, being confined by the cell, will move by the same amount as the cell. The exposures must be short enough so that the particle does not move more than a few microns during the exposure. This will be most easily achieved at the maximum amplitude where the velocity of the particle and cell are at zero. In addition, at this condition the dimension, being at its greatest value, can be measured more accurately. It should be noted that the phase difference between the fluid and the particle is small enough for most cases to be neglected in making the amplitude measurements; however not in all cases. It must be accounted for in some cases.
2. In two different recordings, record the two positions of the particle and a reference point on the cell as in the first method. Registration is required between the two different recordings to make measurements of changes that took place in the time between the recordings.

The particle and cell positions or amplitudes must be determined with an accuracy of 5 microns. It would be beneficial to do better than this, say one to two microns. The particle and cell positions can be determined by locating edges or centroids.

Locating the edge of a focused microscopic image produced by the hologram with the required accuracy is a relatively straightforward procedure; however, with electronic (CCD) images, the problem is different. Typically, the 10 microns pixels are the limiting factor, and sub pixel resolution requires additional image handling and processing. Sub pixel imaging is more easily achieved on a distributed light pattern such as an out of focus image or a diffraction pattern. Figure 3 shows a diffraction pattern of a 1 mm radius magnesium sphere suspended in Krytox. By performing a cross correlation between two recordings of this pattern, which is distributed over many pixels, the center of the Poisson's pattern can be located to a small fraction of a pixel. We found that the portion of the diffraction pattern in the shadow of the particle that contains the Poisson's spot, shown in the top right of the photo, provides an excellent noise free, predictable light pattern (shown in the bottom right) that can be used as a correlation template with both single and double exposure recordings. The correlation templated is then cross-correlated with the single or double exposures, giving a correlation peak at the center of each diffraction pattern in the recording.

Figure 4 shows an actual correlation peak produced by correlating a template produced from the diffraction pattern with the diffraction pattern, showing the center position location through interpolation to better than 0.1 pixels.

The Tethered Particle Method

A fiber was attached to the particle, which is then held in the center of the cell, by attaching the other end of the hair to the bottom of the cell (or the top for heavy particles). This method proved useful especially for large particles.

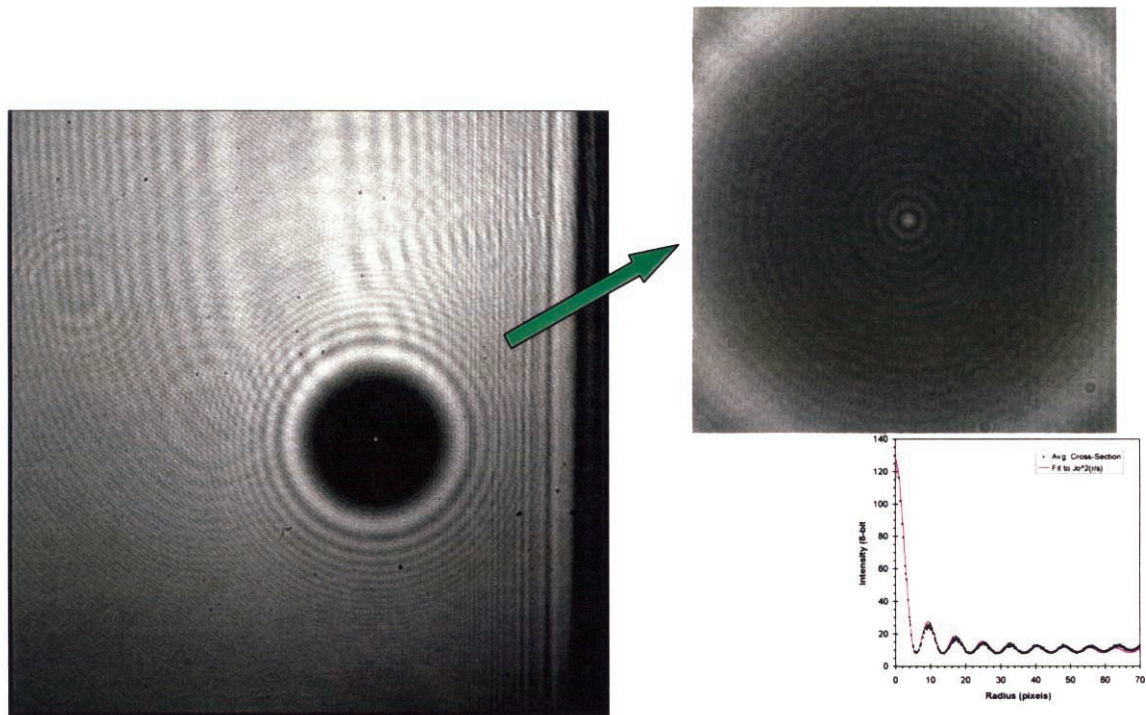


Figure 3. Fresnel Diffraction Pattern of a 1 mm Radius Sphere, showing the Poisson's spot and pattern and theoretical intensity distribution.

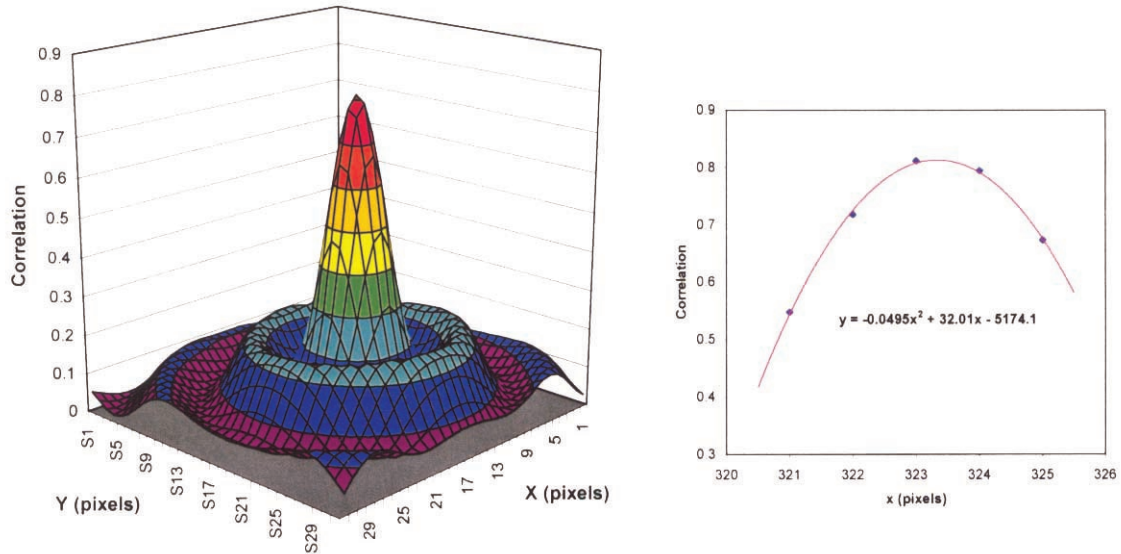


Figure 4. Cross-correlation of a template with the diffraction pattern in Figure 3. The curve on the right hand side shows that the center of the correlation can be located through interpolation with sub pixel accuracy.

Figure 5 shows a tethered 1 mm radius polypropylene particle tethered on a 100-micron diameter fiber. In this figure, the holograms are recorded at two times, when the sphere is located at extremes of the vibration. With this configuration, we have been able to examine many different types of particles, particle interactions, and particle wall interactions.

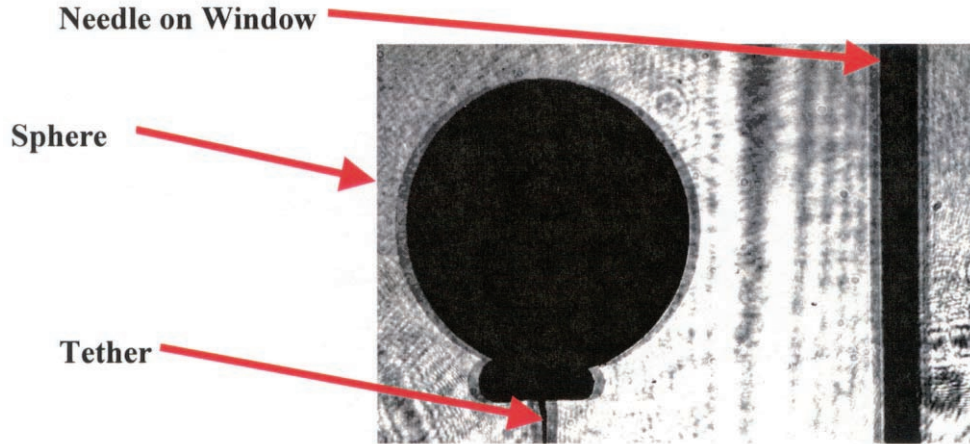


Figure 5. A 1 mm tethered sphere undergoing vibration.

Figure 6 shows a plot of the amplitude of particle motion to fluid motion at various amplitudes for a free particle. The slope of this line provides the predicted parameter, η . By taking several points on the curve to produce this value, the accuracy can be improved considerably to even better than what would be provided with the best position accuracy at a single point. The predicted value in these cases was within 1% of the measured value.

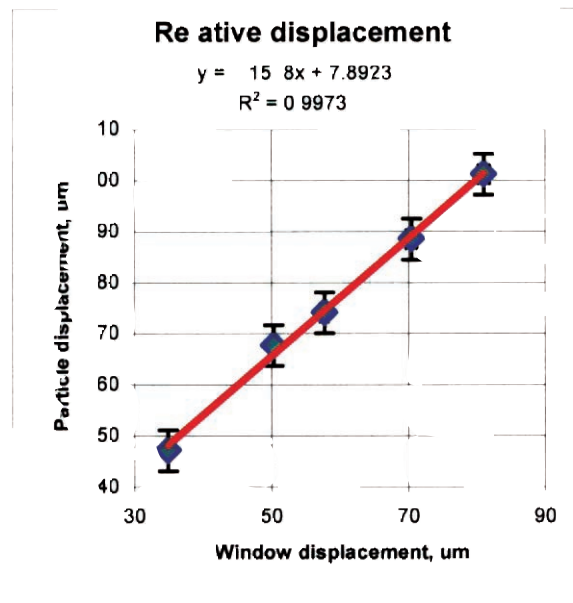


Figure 6. Ratio of particle to fluid displacement at 60 Hz vibration. The important number is the slope, or 1.1518. This number falls within 1% of the value predicted by the Coimbra-Rangel solution. The parameter $S=1$, and $\alpha=2$.

We took data for a range of vibration amplitudes over a frequency range from 30 to 80 Hz. for a tethered 1mm radius sphere. Figure 7 shows a frequency sweep at three different amplitudes of a tethered 1mm radius sphere. Note that the ratios are significantly smaller than the case of the free particle, suggesting the effect of the tether on the particle motion is not negligible for this case.

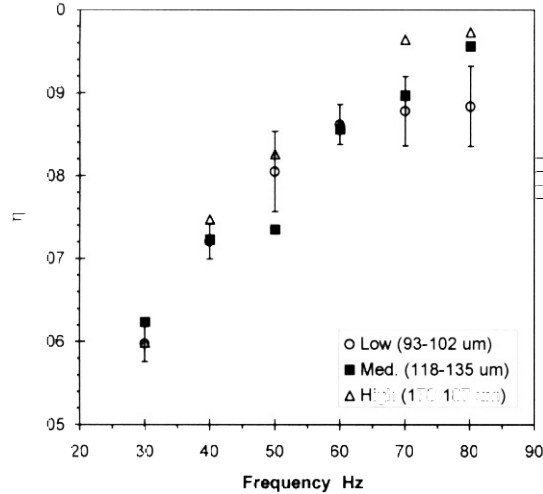


Figure 7. Plot of ratio $\eta = Ap/Ac$ vs. cell oscillation frequency for polypropylene particle in krytox ($\alpha=1.1$). The particle was located near the center of the cell, and did not interact with the walls. Three different data sets are shown for three Ac ranges: low amplitude ($Ac = 93-102 \mu\text{m}$), medium amplitude ($Ac=118-135 \mu\text{m}$), and high amplitude ($Ac=178-187 \mu\text{m}$). Uncertainty bars for η are plotted for the low amplitude data set. The uncertainty in the frequency is typically 0.2 Hz.

Experiments include particles interacting with walls and other particles. Figure 8 shows the results of an experiment designed to examine the effect interaction between the cell wall and the particle. In this experiment, the center of the polypropylene particle was 5.2 mm away from the wall. At each frequency, the ratio η was greater for the wall-interacting particle than for the non-interacting particle, an unexpected result.

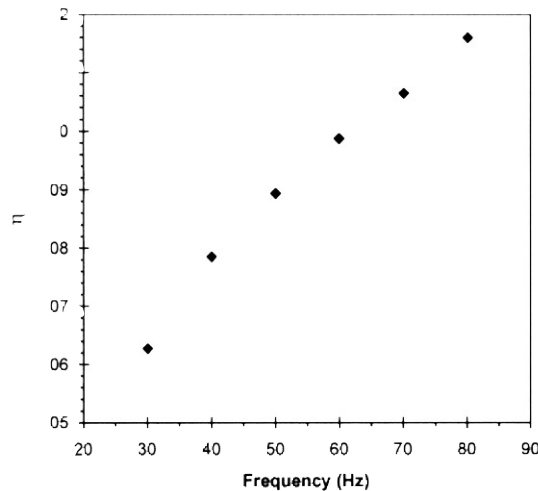


Figure 8. Plot of ratio $\eta = Ap/Ac$ vs. cell oscillation frequency for a polypropylene particle in krytox ($\alpha=2.1$) whose center is 5.2 mm from a wall. Ac ranged from 125 to 142 microns. For a given frequency, η is higher for the wall-interacting particle than for the non-interacting particle. The uncertainties in η and frequency are approximately the same as those in figure 3. Each point represents the average of 10 separate measurements.

Figure 9 shows the results of an experiment designed to examine the effect of oscillation frequency on the motion of a steel particle in krytox ($\alpha=.24$). Because steel is denser than krytox, the particle displacement is always less than the cell displacement. As the frequency increases, η decreases.

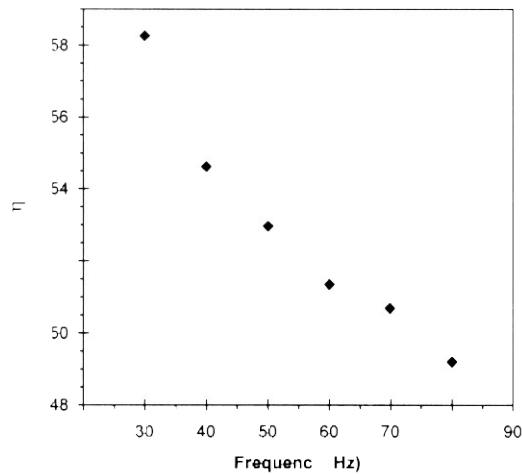


Figure 9. Plot of ratio $\eta=A_p/A_c$ vs. cell oscillation frequency for a steel particle in krytox ($\alpha=.24$). The particle was located near the center of the cell, and did not interact with the walls. A_c ranged from 138 to 149 μm .

Figure 10 shows a plot of η versus frequency for a magnesium alloy particle in krytox ($\alpha =1.10$). The theory predicts that η should be slightly greater than 1 for this particle, however, we observe the surprising result that all values of η are less than 1. The discrepancy may be due to the drag created by the tether, which would slow the particle and reduce A_p . The effect of tether drag on particles is strongest for particles whose density matches that of the fluid. We will conduct some free particle experiments to confirm this result.

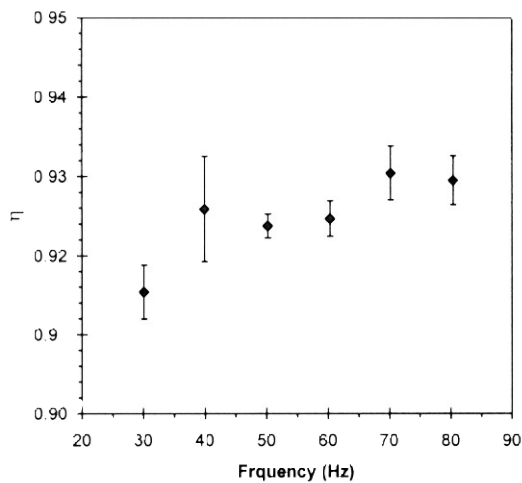


Figure 10. Plot of ratio $\eta=A_p/A_c$ vs. cell oscillation frequency for a magnesium alloy particle in krytox ($\alpha=1.10$). The particle was located near the center of the cell, and did not interact with the walls. A_c ranged from 116 to 138 μm . Uncertainty bars for η are plotted.

The theory predicts that the particle and cell are slightly out of phase, and that a particle with $\alpha = 2$ will reach its extreme of motion a fraction of a millisecond before the cell does. To pinpoint the extremes of particle motion, a series of recordings were made where the first illumination pulse coincided with one extreme of the cell motion, and the delay between the first and second pulses was varied. Figure 11 shows a plot of A_c and A_p versus the time delay between illumination pulses for a cell oscillating at 60.0 Hz. The maximum cell displacement is observed when the time delay is 8.3 ms, which corresponds to one half the oscillation period. The maximum particle displacement is observed at a time delay of 8.0 ms, or 0.3 ms earlier than the cell, which corresponds to a phase difference of 7 ± 2 degrees.

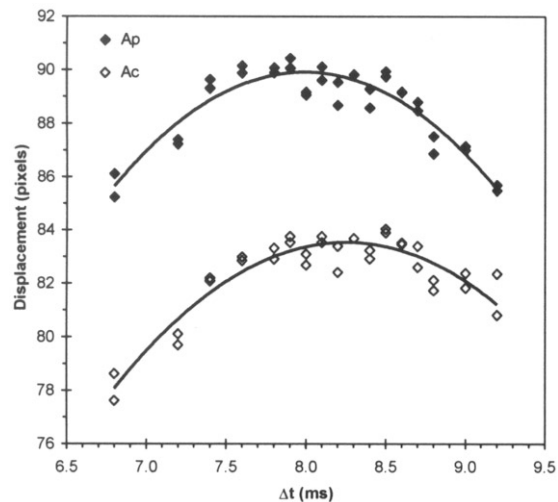


Figure 11. Plots of A_p (black diamonds) and A_c (white diamonds) versus the time between light pulses (Δt) for a polypropylene particle in krytox ($\alpha=0.48$). The cell oscillation frequency was 60.0 ± 0.1 Hz. Each plot is fit by a quadratic polynomial ($A = a\Delta t^2 + b\Delta t + c$). The largest cell displacement is observed when $\Delta t=8.3$ ms, while the largest particle displacement is observed when $\Delta t=8.0$ ms. The uncertainty in the displacements is approximately 1 pixel, which corresponds to $1.8 \mu\text{m}$.

Conclusions

In the foregoing, we have presented some results of a ground based experimental program that is designed to support the flight experiment SHIVA. We have proven that we can determine the position of a particle and fluid with sufficient accuracy to test the analytical solutions of the general equations of motion of a particle in a fluid. We have verified the solutions for a limited range of experimental parameters that can be met on earth. We have used a tethered particle method to simulate microgravity in the conduct of a wider range of parameters. Our preliminary experiments have shown that the tethering fiber does affect particle movement and we continue to search for methods that reduce tether effects.

Acknowledgments

This is a NASA flight definition NRA (NAS8-98091) under topic NRA-96 HEDS-02. The NASA management team includes Melanie Bodiford, Project Manager, Dr. David Smith, Project Scientist, Bill Patterson, Systems Engineer, all from Marshall Space Flight Center. The authors wish to acknowledge Michael Dempsey of MetroLaser for conducting much of the experimental work.

References

1. Coimbra, C.F.M., and Rangel, R.H. "General Solution of the Particle Momentum Equation in Unsteady Stokes Flows." *J. Fluid Mech.*, **370**, 53-72 (1998).

2. Roger H. Rangel, James D. Trolinger, Carlos F. M. Coimbra, Jose Castillo, Carlos Torres, “Studies Of Fundamental Particle Dynamics In Microgravity” UEF: MTP-01-32 Proceedings of the Microgravity Transport Processes in Fluid, Thermal, Biological and Materials Sciences II, Banff, Alberta, Canada, September 30 - October 5, 2001.
3. J.D. Trolinger, C.F.M. Coimbra, R.H. Rangel, W.K. Witherow, and J. Rogers, Studies of Fundamental Particle Dynamics in Microgravity; Second Pan-Pacific Basin Workshop; Pasadena, CA; 1-4 May 2001.